

---

## Research Paper

---

# Raffinose Crystallization During Freeze-Drying and Its Impact on Recovery of Protein Activity

Koustuv Chatterjee,<sup>1,3</sup> Evgeniy Y. Shalaev,<sup>2</sup> and Raj Suryanarayanan<sup>1,4</sup>

Received September 14, 2004; accepted November 8, 2004

**Purpose.** To study i) phase transitions in raffinose solution in the frozen state and during freeze-drying and ii) evaluate the impact of raffinose crystallization on the recovery of protein activity in reconstituted lyophiles.

**Methods.** X-ray powder diffractometry (XRD) and differential scanning calorimetry (DSC) were used to study the frozen aqueous solutions of raffinose pentahydrate. Phase transitions during primary and secondary drying were monitored by simulating the entire freeze-drying process, *in situ*, in the sample chamber of the diffractometer. The activity of lactate dehydrogenase (LDH) in reconstituted lyophiles was determined spectrophotometrically.

**Results.** Raffinose formed a kinetically stable amorphous freeze-concentrated phase when aqueous solutions were frozen at different cooling rates. When these solutions were subjected to primary drying without annealing, raffinose remained amorphous. Raffinose crystallized as the pentahydrate when the solutions were annealed at a shelf temperature of  $-10^{\circ}\text{C}$ . Primary drying of these annealed systems resulted in the dehydration of raffinose pentahydrate to an amorphous phase. The phase separation of the protein from the amorphous raffinose in these two systems during freeze-drying resulted in a significant reduction in the recovery of LDH activity, even though the lyophile was amorphous.

**Conclusions.** Annealing of frozen aqueous raffinose solutions can result in solute crystallization, possibly as the pentahydrate. The crystalline pentahydrate dehydrates during primary drying to yield an amorphous lyophile. Raffinose crystallization during freeze-drying is accompanied by a significant loss of protein activity.

**KEY WORDS:** annealing; freeze-drying; LDH; protein activity; raffinose.

## INTRODUCTION

Lyoprotection, or stabilization of proteins during freeze-drying and storage, is an area of increasing interest in light of the recent advances in recombinant protein pharmaceuticals. Sucrose and trehalose have extensively been used as lyoprotectants. Nonreducing sugars are crucial to protein stabilization because of their ability to form amorphous freeze-concentrates without initiating Maillard reactions. The two widely reported mechanisms for protein stabilization are i) glass dynamics (nonspecific restriction of conformational flexibility of the protein) and ii) specific hydrogen bonding interactions between the sugar and the protein outer surface that maintains the "native" structure (1). Irrespective of the actual mechanism of protein stabilization, there is a common requirement that the protective solutes (sugars) have to be retained amorphous during freeze-drying to form a single amorphous phase with the protein, without phase separation or demixing (1). Sucrose and trehalose are suitable models in

this respect and their stability in the amorphous state has been well documented (2,3). Under optimal conditions, both sugars do not crystallize in the experimental timescale of freeze-drying, nor do they crystallize during storage.

Raffinose, a trisaccharide containing galactose and sucrose, has been the subject of few investigations (4,5). The stoichiometric water content in raffinose pentahydrate ( $\text{C}_{18}\text{H}_{32}\text{O}_{16}\cdot 5\text{H}_2\text{O}$ ) is higher than that in any other carbohydrate used as a lyoprotectant. Dehydration experiments suggested the possibility of several states of hydration, though powder X-ray diffractometry did not enable unambiguous distinction between the hydrates (6). The single-crystal structure of raffinose pentahydrate has recently been revisited, and it appears that two of the five water molecules are present in channels (5). The ready loss of two water molecules on dehydration suggests that the trihydrate can be formed without any appreciable change in lattice structure. Drying under more severe conditions, for example in a vacuum oven at  $60^{\circ}\text{C}$  for 24 h, yielded an amorphous anhydrate (4). Finally, raffinose has also been reported to be the most fragile of all commonly used nonreducing sugars, which makes it a potentially strong lyoprotectant (6). However, unlike sucrose and trehalose, amorphous raffinose has a strong tendency to crystallize during freeze-drying (7). Therefore, when designing a lyophilized protein formulation containing raffinose, it is important to avoid the conditions under which it can crystallize.

<sup>1</sup> College of Pharmacy, University of Minnesota, Minneapolis, Minnesota 55455, USA.

<sup>2</sup> Pfizer Groton Laboratories, Groton, Connecticut 06340, USA.

<sup>3</sup> Current address: Amgen Inc., Thousand Oaks, California 91320, USA.

<sup>4</sup> To whom correspondence should be addressed. (e-mail: surya001@tc.umn.edu)

The existence of amorphous raffinose in the lyophile does not guarantee that crystallization did not occur *during* freeze-drying. The dehydration behavior of disodium hydrogen phosphate dodecahydrate during freeze-drying was recently reported (8). When an aqueous solution of disodium hydrogen phosphate was cooled, it crystallized as the dodecahydrate ( $\text{Na}_2\text{HPO}_4 \cdot 12\text{H}_2\text{O}$ ). Interestingly, it dehydrated during primary drying yielding an amorphous anhydrate. It is thus of practical interest to investigate the phase behavior of raffinose pentahydrate solution in frozen solutions and during freeze-drying. The reported crystallization tendency of raffinose during freeze-drying needs to be investigated in detail. Crystallization of solutes during freeze-drying can be influenced by many factors, namely solute concentration, cooling rate, annealing time and temperature, and primary drying conditions. Solute concentration is potentially an important factor in raffinose crystallization, since the aqueous solubility of raffinose at room temperature is ~16% w/v (9), which is significantly less than that of sucrose or trehalose. Thus if a concentrated raffinose solution (close to saturation at room temperature) is cooled, supersaturation can result in nucleation. The effect of phase separation on protein activity can be studied with a suitable model that is inherently susceptible to lyophilization-induced inactivation. Based on this criterion, lactate dehydrogenase (LDH) was selected for testing post-lyophilization recovery of protein activity. It undergoes irreversible unfolding during freeze-drying; hence assay of reconstituted lyophiles provide useful information about loss of activity during the freeze-drying cycle (10).

Therefore, the objectives of this study are i) to investigate phase transitions in aqueous raffinose systems in frozen solutions and during freeze-drying as a function of processing variables and ii) to study the impact of raffinose crystallization during freeze-drying on the recovery of activity of a model protein.

## MATERIALS AND METHODS

Raffinose pentahydrate ( $\text{C}_{18}\text{H}_{32}\text{O}_{16} \cdot 5\text{H}_2\text{O}$ ; D+,  $\geq 99\%$ ), citric acid (anhydrous), trisodium citrate, and L-lactic dehydrogenase (lyophilized powder-M4 isoenzyme, from rabbit muscle, MW ~142 kDa), were all purchased from Sigma (St. Louis, MO, USA) and used as received. Sodium pyruvate and  $\beta$ -nicotinamide adenine dinucleotide (reduced NADH, disodium hydrate, 25 mg vial) were also purchased from Sigma and used for LDH assay.

### Solutions

Aqueous solutions of raffinose pentahydrate at concentrations of 5%, 10%, and 14% w/v were prepared by dissolving appropriate amounts of raffinose pentahydrate in water. The prelyo protein solution was prepared using lyophilized LDH (final concentration 20  $\mu\text{g}/\text{ml}$ ), buffered with anhydrous citric acid and trisodium citrate (20 mM total buffer concentration) and contained 5%, 10%, or 14% w/v raffinose pentahydrate. The solutions were filtered (0.45  $\mu\text{m}$ ) before lyophilization and DSC or XRD analysis.

### Differential Scanning Calorimetry

A differential scanning calorimeter (MDSC, model 2920, TA Instruments, New Castle, DE, USA) equipped with a

refrigerated cooling accessory was used. An empty aluminum pan was used as a reference. About 10–15 mg of aqueous solution was weighed into an aluminum pan, crimped hermetically, and cooled from room temperature to  $-60^\circ\text{C}$  at  $10^\circ\text{C}/\text{min}$ . It was held isothermally for 5 min, and then heated to room temperature under a stream of nitrogen, at  $5^\circ\text{C}/\text{min}$ . When annealing was required, it was carried out isothermally at  $-10^\circ\text{C}$  for 5 h. After annealing, the solutions were cooled to  $-60^\circ\text{C}$  at  $10^\circ\text{C}/\text{min}$ , and rewarmed. More specific details are provided in the “Results” and “Discussion” sections.

### X-Ray Powder Diffractometry

An X-ray powder diffractometer (model XDS 2000, Scintag, Cupertino, CA, USA) with a variable temperature stage (Micristar, model 828D, R.G. Hansen & Associates, Santa Barbara, CA, USA; working temperature range  $-190^\circ\text{C}$  to  $300^\circ\text{C}$ ) was used. The temperature stage of the X-ray powder diffractometer was attached to a vacuum pump. As a result it was possible to simulate the entire freeze-drying process in the sample chamber of the X-ray powder diffractometer. Although the general details are provided here, the specific experimental conditions are discussed in the “Results” and “Discussion” sections. An accurately measured amount of solution (100  $\mu\text{l}$ ) was filled into a copper sample holder and cooled at either 1 or  $10^\circ\text{C}/\text{min}$  to  $-70^\circ\text{C}$ . When quench cooling was desired, the X-ray holder containing the solution was dipped into a bath of liquid nitrogen and transferred to the X-ray powder diffractometer stage, which was precooled to  $-90^\circ\text{C}$  at  $10^\circ\text{C}/\text{min}$ . The frozen solutions were then heated to  $-30^\circ\text{C}$  at  $5^\circ\text{C}/\text{min}$ . X-ray diffraction (XRD) patterns were obtained by exposing the sample to Cu  $\text{K}\alpha$  radiation (45 kV  $\times$  40 mA), where the scanning speed and the step size were  $5^\circ/2\theta/\text{min}$  and  $0.03^\circ 2\theta$ , respectively. During the XRD runs, isothermal conditions were maintained. Primary drying was carried out at  $-30^\circ\text{C}$ , at a chamber pressure of ~100 mTorr until all the crystalline ice was removed. It was then heated to the secondary drying temperature of  $20^\circ\text{C}$ . Selected samples were annealed at  $-10^\circ\text{C}$  for 8 h before the primary drying step. After annealing, the solutions were cooled to  $-30^\circ\text{C}$  for primary drying.

### Freeze-Drying

Freeze-drying was carried out in a bench top (Advantage, Virtis, Gardiner, NY, USA) freeze-drier. The solutions were filled in 10 ml vials (Wheaton, type I borosilicate glass, Millville, NJ, USA), placed on the shelf of a freeze-dryer and cooled from room temperature to  $-40^\circ\text{C}$  at  $<1^\circ\text{C}/\text{min}$  and held for 4 h. The frozen samples were then heated to  $-30^\circ\text{C}$  at  $0.5^\circ\text{C}/\text{min}$ , the chamber pressure reduced to 70 mTorr, and primary-dried for 35 h. The samples were then heated to  $30^\circ\text{C}$  at  $0.1^\circ\text{C}/\text{min}$  and secondary-dried for 20 h. Selected samples were annealed at  $-10^\circ\text{C}$  for 8 h before the primary drying step following which they were cooled back to  $-30^\circ\text{C}$  for primary drying. The product temperature was  $-5$ – $8^\circ\text{C}$  lower than the shelf temperature at all times during primary drying. One set of annealed samples was primary-dried for a shorter duration of 25 h. More specific details will be addressed in the “Results” and “Discussion” sections. On completion of the process, the vials were stoppered (gray butyl 20 mm corkage, VWR) in vacuum. The vials were stored in the refrigerator and analyzed within 72 h.

## LDH Assay

The lyophiles containing LDH were reconstituted with 5 ml of distilled water. The enzymatic assay method is based on the reversible reaction between lactate and pyruvate (11). When pyruvate is reduced, an equimolar amount of NADH is oxidized to NAD. The oxidation of NADH results in a decrease in absorbance at 340 nm, the rate of which is directly proportional to LDH activity in the sample. A stock solution containing 80 mM Na-pyruvate and 6 mM NADH was prepared in 20 mM citrate buffer solution. To each assay cuvette (1 cm pathlength) containing 1.94 ml of 20 mM citrate buffer, 100  $\mu$ l of this solution was added. To this substrate, 30  $\mu$ l of the unknown LDH samples was added. Thus the total volume of solution in the cuvette was 2.07 ml. A thermometer was used inside the spectrophotometer chamber to note significant temperature fluctuations, if any. The substrates were prepared fresh during each assay and protected from light, in order to avoid NADH degradation. Standard LDH samples were checked with and without formulation excipients to determine possible interference. From the data acquired in the second minute in one-second intervals, the slope representative of NADH conversion was calculated. Such calculations were first performed for the pre-lyo solution immediately before freeze-drying. After freeze-drying, the slope was again measured on reconstitution of the lyophiles. The ratio of the two slopes would indicate the LDH activity retained, immediately after freeze-drying. All assays were performed in triplicate. This assay is routinely used to measure loss of LDH activity after freeze-drying (12).

## Karl Fischer Titrimetry

At the end of the lyophilization, the vials were sealed under vacuum in the freeze-dryer. Anhydrous methanol was injected into the vials through the rubber stopper and mixed well to obtain a suspension. It was withdrawn into a syringe and a known weight of the suspension was injected into the titration vessel of a Karl Fischer titrimer (model CA-05 Moisture Meter, Mitsubishi). Based on the amount of lyophile in the vial, the quantity of methanol added, and the water content in the methanol blank, the lyophile water content was calculated. All results were acquired in triplicate.

## RESULTS

### Phase Transitions in Raffinose Solutions

The DSC profiles of raffinose solutions (5%, 10%, and 14% w/v) revealed ice formation during cooling and two endothermic step transitions during the warming curve (data not shown). The lower temperature, weaker transition, was at  $-40.3^{\circ}\text{C}$  ( $T_g''$ ) and the higher temperature, stronger transition, was at  $-28.4^{\circ}\text{C}$  ( $T_g'$ ). Because raffinose crystallization was not detected, all solutions were annealed at  $-10^{\circ}\text{C}$  for 5 h, cooled to  $-60^{\circ}\text{C}$  and rewarmed to room temperature. The  $T_g'$  and  $T_g''$  values were unaffected by the annealing step.

In the variable temperature XRD experiments, the effect of cooling rate was first investigated. In addition to quench cooling, the samples were cooled at 10 or at  $1^{\circ}\text{C}/\text{min}$ . There was no evidence of solute crystallization in any of the samples. In an effort to induce solute crystallization, the solutions were annealed. Because sub- $T_g'$  annealing has been reported to

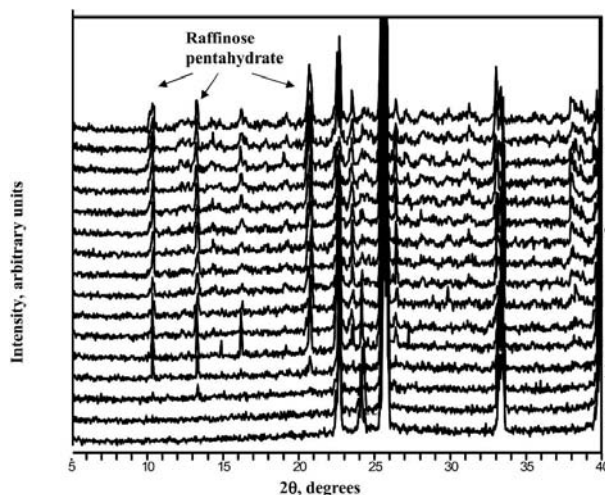


**Fig. 1.** XRD patterns demonstrating crystallization of raffinose pentahydrate during annealing of frozen aqueous raffinose solutions (10% w/v) at  $-10^{\circ}\text{C}$ . The solution was cooled from room temperature to  $-70^{\circ}\text{C}$  at  $10^{\circ}\text{C}/\text{min}$  and then heated to  $-10^{\circ}\text{C}$  at  $5^{\circ}\text{C}/\text{min}$ . Only the crystalline hexagonal ice was evident at  $-10^{\circ}\text{C}$  (peaks at  $22.5$ ,  $24.1$ , and  $25.5^{\circ}2\theta$ ; scan A). The next 8 scans (from bottom upwards) were acquired at intervals of 15 min. The first evidence of raffinose crystallization (peak at  $\sim 13.2^{\circ}2\theta$ ) was observed after 30 min of annealing (scan B). Scans C through D were acquired at intervals of 30 min. The last three scans (scans D through E) were acquired at 1-h intervals. Only selected scans have been labeled. In Fig. 2, the intensities of selected raffinose pentahydrate peaks have been plotted as a function of annealing time.

facilitate mannitol crystallization (13), annealing was carried out at  $-32^{\circ}\text{C}$ . There was no evidence of raffinose crystallization even after annealing for 8 h. When the annealing temperature was increased to  $-10^{\circ}\text{C}$ , at higher raffinose concentrations (10% and 14% w/v), solute crystallization was evident. Figure 1 contains XRD patterns obtained during annealing of frozen raffinose solution (10% w/v). In Fig. 2, the sum of the intensities of two characteristic peaks of raffinose pentahydrate has been plotted as a function of the annealing time. Following a short lag time, the initial crystallization was very rapid. The crystallization appears to plateau after  $\sim 350$  min. When a 5% w/v raffinose solution was annealed at the

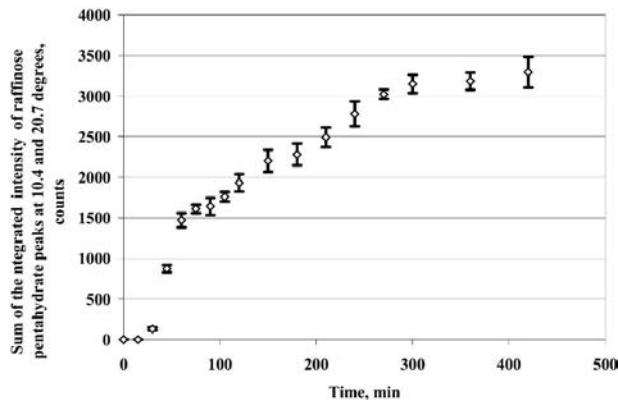


**Fig. 2.** Sum of the integrated intensities of the raffinose pentahydrate peaks at  $10.4$  and  $20.7^{\circ}2\theta$  plotted as a function of annealing time (mean  $\pm$  SD;  $n = 3$ ). The experimental conditions are described in the legend of Fig. 1.

same temperature, the characteristic peaks of raffinose pentahydrate were not observed.

### Phase Transitions During Primary Drying

When frozen unannealed raffinose solutions (5%, 10%, and 14% w/v), were primary-dried at  $-30^{\circ}\text{C}$ , amorphous lyophiles were obtained. To investigate the effect of annealing, these solutions were annealed at  $-10^{\circ}\text{C}$  shelf temperature, followed by primary drying at  $-30^{\circ}\text{C}$ . At a raffinose concentration of 5% w/v, there was no evidence of solute crystallization either during annealing (discussed earlier) or during the primary-drying process. During primary drying, there was a progressive decrease in the intensity of the peaks of hexagonal ice until they disappeared completely, yielding an amorphous product. We had earlier seen that at higher raffinose concentrations of 10% and 14% w/v, annealing resulted in solute crystallization. Interestingly, during primary drying, there was a gradual decrease in peak intensities finally yielding an amorphous product (Fig. 3). Although annealing had caused crystallization of raffinose pentahydrate, the low chamber pressure during primary drying had resulted in a dehydrated reaction yielding an amorphous anhydrous phase. Such a transition of disodium hydrogen phosphate dodecahydrate ( $\text{Na}_2\text{HPO}_4 \cdot 12\text{H}_2\text{O}$ ) to the amorphous anhydrate was observed during primary drying (8). As before, based on the intensity of the characteristic raffinose pentahydrate peaks, it was possible to monitor the dehydration of raffinose pentahydrate as a function of the primary-drying time (Fig. 4).

The results obtained in the variable temperature XRD studies formed the basis for the development of the lyocycle.

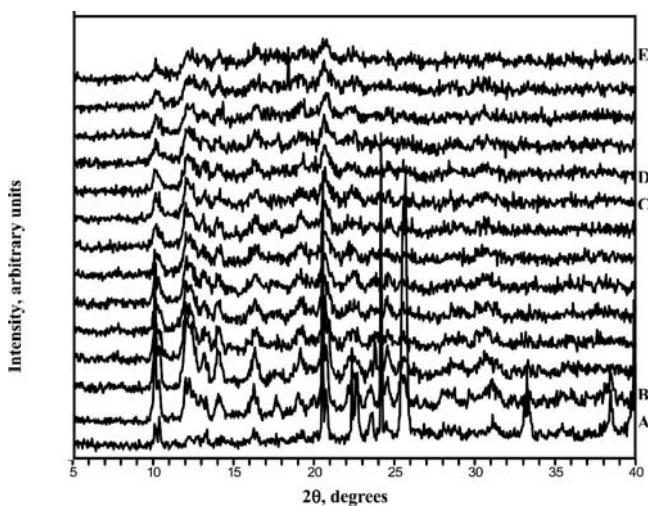


**Fig. 3.** XRD patterns demonstrating dehydration of raffinose pentahydrate during primary drying at  $-30^{\circ}\text{C}$ . The solution (10% w/v) was cooled from room temperature to  $-70^{\circ}\text{C}$  at  $10^{\circ}\text{C}/\text{min}$  and then heated to  $-10^{\circ}\text{C}$  at  $5^{\circ}\text{C}/\text{min}$ . XRD revealed only the crystallization of ice. Annealing at this temperature for 7 h showed substantial raffinose crystallization and the solution was cooled to  $-30^{\circ}\text{C}$  to begin primary drying. The lowermost scan (A) was obtained before primary drying was initiated. Scans B through C were acquired at 15-min intervals (from bottom, upwards), and scans D through E were acquired at 30-min intervals. The product at the end of primary drying was substantially amorphous (scan E). In Fig. 4, the intensities of selected raffinose pentahydrate peaks have been plotted as a function of annealing time.

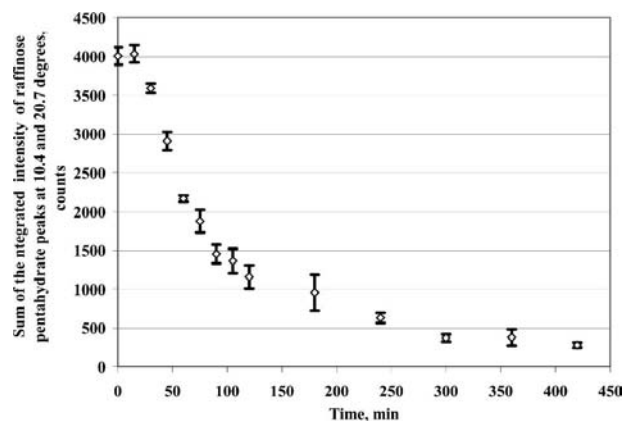


**Fig. 4.** Sum of the integrated intensities of the raffinose pentahydrate peaks at  $10.4$  and  $20.7^{\circ}2\theta$  plotted as a function of primary drying time (mean  $\pm$  SD;  $n = 3$ ). The experimental conditions are described in the legend of Fig. 3.

Because raffinose crystallization was not observed during primary drying without annealing at  $-30^{\circ}\text{C}$ , this process served as the control. Our hypothesis is that in raffinose solutions, at solute concentrations of 10% and 14% w/v, raffinose crystallizes during annealing. As a result of the phase separation, raffinose is no longer an effective lyoprotectant and the protein is partially inactivated. In order to test this hypothesis, freeze-thaw studies were first carried out with raffinose-protein solutions. The solutions were cooled on the shelf of the freeze-drier to  $-40^{\circ}\text{C}$ , and then thawed in a water bath to  $25^{\circ}\text{C}$ . It is readily evident that at all concentrations, raffinose is an effective cryoprotectant (Fig. 5), as freeze-thawing of LDH solutions without a stabilizer is known to cause substantial loss of protein activity (12). Freeze-drying was next carried out at  $-30^{\circ}\text{C}$  without the annealing step. Again, the recovery of the protein activity was independent of the raffinose concentration (Fig. 6). Moreover, at a given raffinose concentration, there was no significant difference in the protein activity between the prelyo solution and the lyophile. Based on variable temperature XRD, we had concluded that there was no raffinose crystallization during freeze-drying, in unannealed systems. Thus the amorphous carbohydrate was an effective lyoprotectant.

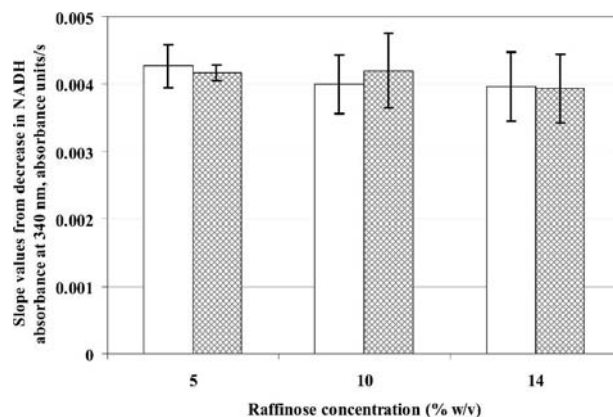


**Fig. 5.** Freeze-thaw studies of LDH solutions ( $20 \mu\text{g}/\text{ml}$ ) with different raffinose concentrations (mean  $\pm$  SD;  $n = 3$ ). Controls are freshly prepared prelyo solutions ( $\square$ ), which were compared with freeze-thawed ( $\boxtimes$ ) solutions.

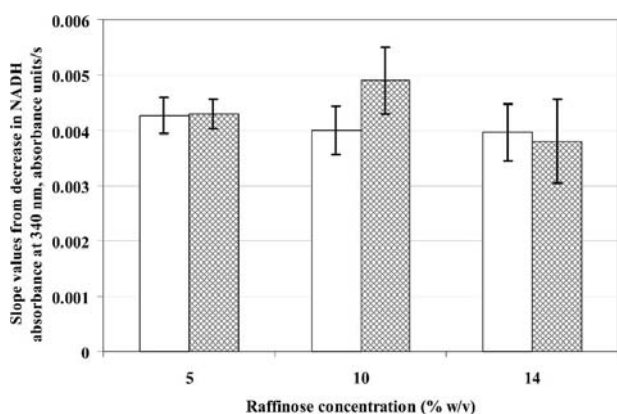


**Fig. 6.** Effect of freeze-drying without the annealing step on the recovery of LDH activity (mean  $\pm$  SD;  $n = 3$ ). Controls are freshly prepared prelyo solutions ( $\square$ ), which were compared with freshly reconstituted lyophilized ( $\boxtimes$ ). Primary drying was carried out at  $-30^{\circ}\text{C}$ .

When the frozen solutions were annealed, a completely different picture emerged. Earlier, in the variable temperature XRD experiments, there was no evidence of raffinose crystallization at a solute concentration of 5% w/v. Expectedly, when these solutions were lyophilized, there appeared to be no loss in protein activity (Fig. 7). However, at higher raffinose concentrations of 10% and 14% w/v, there was a significant decrease in the recovery of protein activity (Fig. 7). Variable temperature XRD experiments had revealed crystallization of raffinose pentahydrate, following the annealing of 10% and 14% w/v raffinose solutions (Fig. 1). The resulting phase separation appears to have caused drying-induced inactivation.

The water content in the lyophilized appeared to be unaffected by the annealing step (Table I; columns 2 and 3). In systems with a higher raffinose concentration (10% or 14% w/v), because raffinose crystallized as the pentahydrate, water was incorporated into the crystal lattice during annealing. The formation of the amorphous anhydrate during primary drying resulted in the release of this water. However, the long secondary drying cycle time of 20 h, effectively removed most of the sorbed water from the system.

One potential benefit of annealing is the reduction in primary drying time, usually by the acceleration of water re-

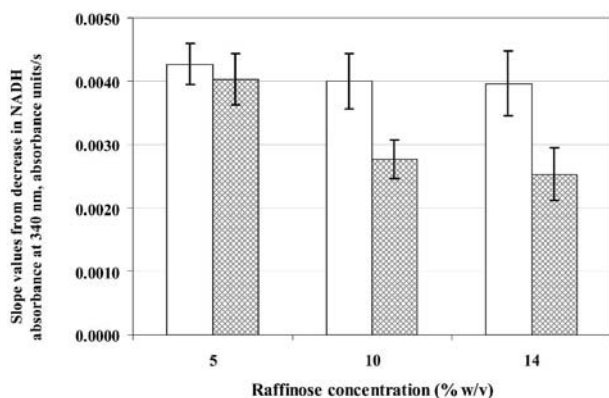


**Fig. 7.** Effect of raffinose concentration on the recovery of LDH activity (mean  $\pm$  SD;  $n = 3$ ) in annealed lyophilized. Controls are freshly prepared prelyo solutions ( $\square$ ), which were compared with freshly reconstituted lyophilized ( $\boxtimes$ ).

**Table I.** Effect of Freeze-Drying Conditions on the Water Content of LDH Lyophilized (Mean  $\pm$  SD;  $n = 3$ )

Raffinose (% w/v)	Primary drying for 35 h followed by secondary drying for 20 h <sup>a</sup>		Primary drying for 25 h; no secondary drying	
	No annealing	Annealing <sup>a</sup>	No annealing	Annealing <sup>b</sup>
5	0.55 $\pm$ 0.06	0.63 $\pm$ 0.11	1.11 $\pm$ 0.13	1.08 $\pm$ 0.06
10	0.61 $\pm$ 0.09	0.71 $\pm$ 0.08	0.96 $\pm$ 0.15	1.76 $\pm$ 0.09
14	0.66 $\pm$ 0.12	0.69 $\pm$ 0.04	1.19 $\pm$ 0.13	1.88 $\pm$ 0.13

The primary and secondary drying temperatures were  $-30^{\circ}\text{C}$  and  $+30^{\circ}\text{C}$ , respectively. Annealing was carried out at  $-10^{\circ}\text{C}$ .

<sup>a</sup> For 5 h at  $-10^{\circ}\text{C}$ .

<sup>b</sup> For 8 h at  $-10^{\circ}\text{C}$ .

moval (14). Thus, it was of interest to examine the effect of the phase transition (hydrate formation during annealing; dehydration during drying) on the water content in the lyophilized after primary drying. The frozen solutions were annealed for 8 h at a shelf temperature of  $-10^{\circ}\text{C}$ , followed by primary drying at  $-30^{\circ}\text{C}$  for 25 h (instead of 35 h as before). The lyocycle was then stopped and the residual water content was measured (Table I, column 5). The experiment was repeated without the annealing step. At higher raffinose content (10% and 14% w/v), primary drying for 25 h appears to be insufficient to remove the released lattice water (columns 4 and 5 in Table I). However, if the secondary drying cycle is long, the final lyophilized water content can be independent of the primary drying conditions.

## DISCUSSION

### Effect of Solute Concentration on Crystallization

According to the classic homogeneous nucleation theory, the nucleation rate  $J$  increases as a function of the degree of supersaturation  $S$  as expressed in Eq. 1 (15):

$$J = A \exp \left[ - \frac{16\pi\sigma^3 v^3 N}{3R^3 T^3 (\ln S)} \right] \quad (1)$$

Here,  $A$  is the collision factor,  $v$  is molecular volume of the embryo,  $\sigma$  is the interfacial energy,  $N$  is the Avogadro number,  $R$  is the gas constant,  $T$  is the absolute temperature, and  $S$  is the degree of supersaturation. Figure 8 shows the raffinose solubility curve that was constructed from the literature data (9). The initial raffinose concentrations were 5.17%, 10.72%, and 15.45% w/w (pointed out in Fig. 8). On cooling these solutions, the higher the initial raffinose concentration, the more rapid was the attainment of saturation (Fig. 8). On further cooling down to  $-70^{\circ}\text{C}$ , the decrease in temperature coupled with ice crystallization, is expected to cause pronounced supersaturation. Interestingly, irrespective of the solute concentration, there was no detectable raffinose crystallization in the frozen solutions. In order to facilitate crystallization, the solutions were annealed at a shelf temperature of  $-10^{\circ}\text{C}$ . Crystallization was only observed when the initial raffinose concentrations were 10.72% and 15.45%

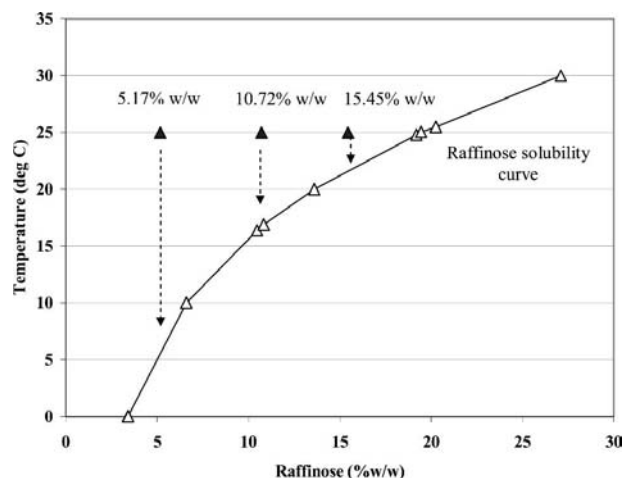


**Fig. 8.** Part of the raffinose-water phase diagram showing the raffinose\* solubility curve ( $\Delta$ ); the data points are taken from the literature (9). (\*Note: Although the results were expressed in terms of anhydrous raffinose, the solid phase in equilibrium with the solution is raffinose pentahydrate). Raffinose solutions at initial concentrations of 5.17%, 10.72%, and 15.45% w/w ( $\blacktriangle$ ) were cooled at  $\sim 1^\circ\text{C}/\text{min}$ . Discontinuous arrows indicate the approach to saturation. On further cooling, the systems readily attained supersaturation, the degree of which depended on the initial raffinose concentration.

w/w (Fig. 1). The degree of supersaturation is expected to be higher in these two systems than when the initial raffinose concentration was 5.17% w/w.

In the frozen and annealed systems, we had expected the extent of raffinose crystallization to be a function of the initial solute concentration. However, the intensity values of the characteristic peaks of raffinose pentahydrate appeared to be independent of the solute concentration (data not shown). Though the nucleation rate would be a function of the supersaturation ratio (Eq. 1), a concomitant increase in viscosity may offset this effect, as was reported in trehalose-mannitol systems (13). The relation between nucleation rate and viscosity can be expressed as (16):

$$J = A' \exp\left(\frac{-\Delta G^* - \Delta G_a}{kT}\right) \quad (2)$$

where  $A'$  is the pre-exponential factor,  $\Delta G^*$  is the Gibbs free energy of cluster formation,  $\Delta G_a$  is the activation energy for transport across the nucleus-liquid interface, and  $k$  is the Boltzmann constant. Because  $\Delta G_a$  is proportional to viscosity, an increase in viscosity would decrease the nucleation rate  $J$ . Thus as the solute concentration increases, the overall nucleation rate will be a balance between supersaturation and viscosity. Although the nucleation characteristics of trehalose can be explained by the theory of homogeneous nucleation, it is recognized that in presence of ice, the secondary crystallization of trehalose is likely to be heterogeneous.

### Annealing in Freeze-Drying

The selection of the annealing temperature will depend on the  $T_g$  of the freeze-concentrated solution. Although there is considerable discussion and controversy regarding the physical origin of the two endothermic step transitions ( $T_g''$  and  $T_g'$ ) in amorphous freeze concentrates, the annealing

temperature was substantially above ( $\sim 18^\circ\text{C}$  to  $30^\circ\text{C}$ ) both values. The crystallization (nucleation and crystal growth) of raffinose can thus be explained from the viewpoint of high mobility at temperatures substantially above  $T_g$ . The upper limit for the annealing temperature would be the raffinose pentahydrate-water eutectic melting temperature of  $-2.75^\circ\text{C}$  (17). Here there is an implicit assumption that low buffer and protein concentrations do not have a substantial impact on the secondary crystallization surface of raffinose and water. If the annealing temperature was very low (close to the glass transition temperature), the very high viscosity would hinder the solute diffusion to form the nuclei. Hence, crystallization of raffinose was not observed when solutions were annealed below  $T_g'$ . On the other hand, at high annealing temperatures (i.e., above the eutectic temperature), the nuclei formed will disintegrate rapidly.

In the XRD, annealing resulted in the appearance of the characteristic peaks of raffinose pentahydrate. However, annealing-induced crystallization was not evident in the DSC. In these two experiments, the samples had been subjected to a similar temperature program. However, the sample size in the XRD ( $\sim 100$  mg) was much larger than that in the DSC ( $\sim 15$  mg). The sample has a pronounced tendency to remain in the supercooled state in the DSC. The influence of sample size on crystallization has been well documented and different mechanisms have been proposed (18). From the perspective of phase behavior during vial lyophilization (typical liquid fill volume is between 1 and 5 ml), data obtained using a large sample size is likely to be most relevant.

There are several examples of lattice collapse (i.e., amorphization) following the removal of water of crystallization from a hydrate. In addition to raffinose pentahydrate (4), dehydration of cefazolin sodium pentahydrate (19) and disodium hydrogen phosphate dodecahydrate (8) during primary drying resulted in the formation of the respective amorphous anhydrides. The water released on dehydration can associate with the amorphous lyophile and have a detrimental effect on the formulation. In the current study, there is an added level of complexity as the amorphous carbohydrate first crystallizes, causing phase separation and protein inactivation. While the subsequent release of water on dehydration has the potential to cause more problems, this was avoided by the prolonged 20-h secondary drying cycle.

Raffinose is known to exist in different states of hydration. The powder X-ray diffraction patterns of the penta-, tetra- and trihydrates of raffinose are virtually identical (6). Thus, powder XRD is not an appropriate technique to identify raffinose in different states of hydration. Because crystallization of raffinose occurs from an aqueous solution, we expect this to be the hydrate with the highest stoichiometric water content (i.e., pentahydrate). However, this claim warrants further verification.

Timasheff had proposed that preferential exclusion of solute (cryoprotectants) stabilizes proteins during freeze thawing (20). Because freezing-induced inactivation is minimal in raffinose-protein systems, the dehydration stresses appear to induce protein instability. Irrespective of the mechanism of stabilization, it is accepted that protein stabilizers need to be amorphous in order to offer lyoprotection. In this study, it was observed that crystallization of a sugar during annealing induced inactivation of the protein.

## CONCLUSIONS

The intention of this article is to shed light on the possibility of phase transitions during freeze-drying and to demonstrate their potential implications on the stability of the active pharmaceutical ingredient. The importance of physical characterization during all the stages of freeze-drying becomes evident. The amorphous state of the stabilizer (lyoprotectant) is a result of the phase transitions that have occurred during the process and do not reflect its physical state during the entire lyophilization process. Often, an annealing step is introduced in an effort to optimize the lyocycle. However, in this system, annealing facilitated the crystallization of the stabilizer and resulted in loss of protein activity. If the XRD pattern of the final lyophile serves as the only proof of the amorphous nature of the stabilizer, it can result in erroneous conclusions. This is clearly observed in the study as the hydration-dehydration phenomenon during freeze-drying resulted in phase separation-induced protein inactivation, though the final lyophiles was X-ray amorphous.

## ACKNOWLEDGMENTS

We thank Dr. John Carpenter for guidance in the protein assay and the Characterization Facility for use of the X-ray powder diffractometer.

## REFERENCES

1. M. J. Pikal. Mechanisms of protein stabilization during freeze-drying and storage: the relative importance of thermodynamic stabilization and glassy state relaxation dynamics. *Drugs Pharm. Sci.* **96**:161–198 (1999).
2. A. Saleki-Gerhardt and G. Zografí. Non-isothermal and isothermal crystallization of sucrose from the amorphous state. *Pharm. Res.* **11**:1166–1173 (1994).
3. O. S. McGarvey, V. L. Kett, and D. Q. M. Craig. An investigation into the crystallization of  $\alpha,\alpha$ -trehalose from the amorphous state. *J. Phys. Chem. B* **107**:6614–6620 (2003).
4. A. Saleki-Gerhardt, J. G. Stowell, S. R. Byrn, and G. Zografí. Hydration and dehydration of crystalline and amorphous forms of raffinose. *J. Pharm. Sci.* **84**:318–323 (1995).
5. K. Kajiwara, A. Motegi, M. Sugie, F. Franks, S. Munekawa, T. Igarashi, and A. Kishi. Studies on raffinose hydrates. In H. Levine (ed.), *Amorphous Food and Pharmaceutical Systems*, Royal Society of Chemistry, Cambridge, 2002, pp. 121–130.
6. K. Kajiwara, F. Franks, P. Echlin, and A. L. Greer. Structural and dynamic properties of crystalline and amorphous phases in raffinose-water mixtures. *Pharm. Res.* **16**:1441–1448 (1999).
7. P. Davidson and W. Q. Sun. Effect of sucrose/raffinose mass ratios on the stability of co-lyophilized protein during storage above the Tg. *Pharm. Res.* **18**:474–479 (2001).
8. A. Pyne, K. Chatterjee, and R. Suryanarayanan. Dehydration of crystalline buffer salt during primary drying. *Pharm. Res.* **20**:802–803 (2003).
9. E. H. Hungerford and A. R. Nees. Raffinose preparation and properties. *Ind. Eng. Chem* **26**:462–464 (1934).
10. J. F. Carpenter, B. S. Chang, W. Garzon-Rodriguez, and T. W. Randolph. Rational design of stable lyophilized protein formulations: theory and practice. In J.F. Carpenter and M.C. Manning (eds.), *Pharmaceutical Biotechnology, Volume 13*, Kluwer Academic/Plenum Publishers, New York, 2002, p. 203.
11. H. U. Bergmeyer and E. Bernt. Lactate dehydrogenase. In H.U. Bergmeyer (ed.), *Methods of Enzymatic Analysis*, Academic Press, London, 1965, pp. 574–579.
12. T. J. Anchordoquy, K. Izutsu, T. W. Randolph, and J. F. Carpenter. Maintenance of quaternary structure in the frozen state stabilizes lactate dehydrogenase during freeze-drying. *Arch. Biochem. Biophys.* **390**:35–41 (2000).
13. A. Pyne, R. Surana, and R. Suryanarayanan. Crystallization of mannitol below Tg' during freeze-drying in binary and ternary aqueous systems. *Pharm. Res.* **19**:901–908 (2002).
14. J. A. Searles, J. F. Carpenter, and T. W. Randolph. Annealing to optimize the primary drying rate, reduce freezing-induced drying rate heterogeneity, and determine Tg' in pharmaceutical lyophilization. *J. Pharm. Sci.* **90**:872–887 (2001).
15. J. W. Mullin and C. L. Leci. Nucleation characteristics of aqueous citric acid solutions. *J. Cryst. Growth.* **5**:75–76 (1969).
16. D. Turnbull and J. C. Fisher. Rate of nucleation in condensed systems. *J. Chem. Phys.* **17**:71–73 (1949).
17. K. Kajiwara and F. Franks. Crystalline and amorphous phases in the binary system water-raffinose. *J. Chem. Soc. Far. Trans.* **93**:1779–1783 (1997).
18. D. Turnbull. Correlation of liquid-solid interfacial energies calculated from supercooling of small droplets. *J. Chem. Phys.* **18**:769 (1950).
19. A. Pyne and R. Suryanarayanan. The effect of additives on the crystallization of cefazolin sodium during freeze drying. *Pharm. Res.* **20**:283–291 (2003).
20. S. N. Timasheff. Water as ligand: preferential binding and exclusion of denaturants in protein unfolding. *Biochem* **31**:9857–9864 (1992).